Little Ambergris Cay, a Case Study for Ooid Rich Island Development on the Turks and Caicos Carbonate Platform

By

Drew G. Brown
Geological Sciences, University of Colorado at Boulder

Defense Date (November 4th, 2020)

Thesis Advisor:

Dr. Elizabeth Trower, Geology

Defense Committee:

Dr. Elizabeth Trower, Geological Sciences
Dr. Brian Hynek, Geological Sciences
Dr. Julia Moriarty, Atmospheric and Oceanic Sciences

Abstract:

Little Ambergris Cay (LAC) within the Turks and Caicos is a useful field site to examine the accumulation of a carbonate island, within a typical carbonate platform environment, because it does not follow the typically accepted modes of island accretion. There are several methods used to describe carbonate island formation after Schlager (2003), who described carbonate “factories” in reference to the modern analogues of Florida and the Bahamas. The Turks and Caicos, and specifically Little Ambergris Cay, offers a field side that differs from the comparison analogues in sediment composition, energy flux, and Holocene development. Little Ambergris Cay is unusual in that it formed during a period of sea level rise (Figure 2, Toscano & Macintyre, 2003), and thus presents an opportunity for research on how modern carbonate platform environments accumulate through time. This paper presents an argument for eastward direction of island accumulation of Little Ambergris Cay. Based on the research of Trower et al. (2018), Dravis & Wanless (2008), and Schlager (2003), I interpret that Little Ambergris Cay formed via eastward accumulation based on the influence of wind-wave current energy as means of supplying ample sediment to a zone of accumulation; in other words, in this system, sediment supply outpaces accommodation space. To support this interpretation, I will present several sets of data that were derived from unlithified sediment cores collected from the interior of LAC as means to characterize and compare against representative environments. First, I performed thin section point-count analysis on loose sediments from a variety of depths in a representative collected core to identify how grain composition varied with depth. I then compared this point count data with a range of grain characteristics such as grain size, sorting, sphericity, etc., determined via Camsizer analysis, in order to determine the parameters that best described the changes in grain concentration as seen in the point count. Finally, by integrating plots of the grain size parameters determined in this paper vs. depth, stereoscope microscopy, and radiocarbon ages of core sediments, I compared representative facies of modern carbonate environments to determine a facies development through time of Little Ambergris Cay. I concluded that Little Ambergris Cay underwent a series of high to low energy facies changes, where early lithification on the south-western edge of the modern LAC allowed successive accumulation of incoming easterly ooids due to sediment entrapment, possibly due to microbial mat and bedrock influence. The incoming sediment grains from the east onto an early lithified fragment to the west allowed eastward accumulation, where facies changed from an ancient shoal to a modern island. This paper furthers the research of modern carbonate analogues and their interpreted growth patterns. LAC offers a unique environment that does not follow typical carbonate island development, and by providing a case study of wind-wave influenced island accretion, sectors of geologic interest have the opportunity to interpret unique climatic and chemical factors. The petroleum unconventional subsurface carbonate play search is greatly related to LAC, as grainstones offer potential reservoirs (Dravis & Wanless, 2008). The geochemical field may have interest in the accumulation of LAC, as specific seawater concentrations play a role in the uniquely high concentrations of ooids found on the Caicos Platform. The geobiological field may be interested in LAC, as the relatively low abundance of microbes and biotic influence differs greatly from the other modern analogues for carbonate platform development.

Introduction:

Little Ambergris Cay (LAC, Figure 1) within the Turks and Caicos is known to be composed of dominantly Holocene aged carbonate sediments (Orzechowski et al., 2016). Toscano & Macintyre (2003) recognized that a period of sea level rise occurred in the Atlantic Holocene. Generally speaking, using the Bahamas and Florida as a modern analogue for carbonate platform development, the most common way for carbonate accumulation to outpace or remain at increasing sea level is through a process of “backstepping,” or retrogradation of the platform that is primarily influenced by reef growth (Schlager, 2003). Reefs are rare on the Caicos platform, so considering that we instead primarily observe Holocene ooids (Dravis and Wanless, 1989), and recognizing that LAC accreted past sea level during a period of increasing accommodation space, it then becomes clear that LAC does not follow the most obvious modern models of island formation in the Holocene. This anomaly offers an opportunity to better understand how and why formation of this carbonate platform island occurred in such conditions.

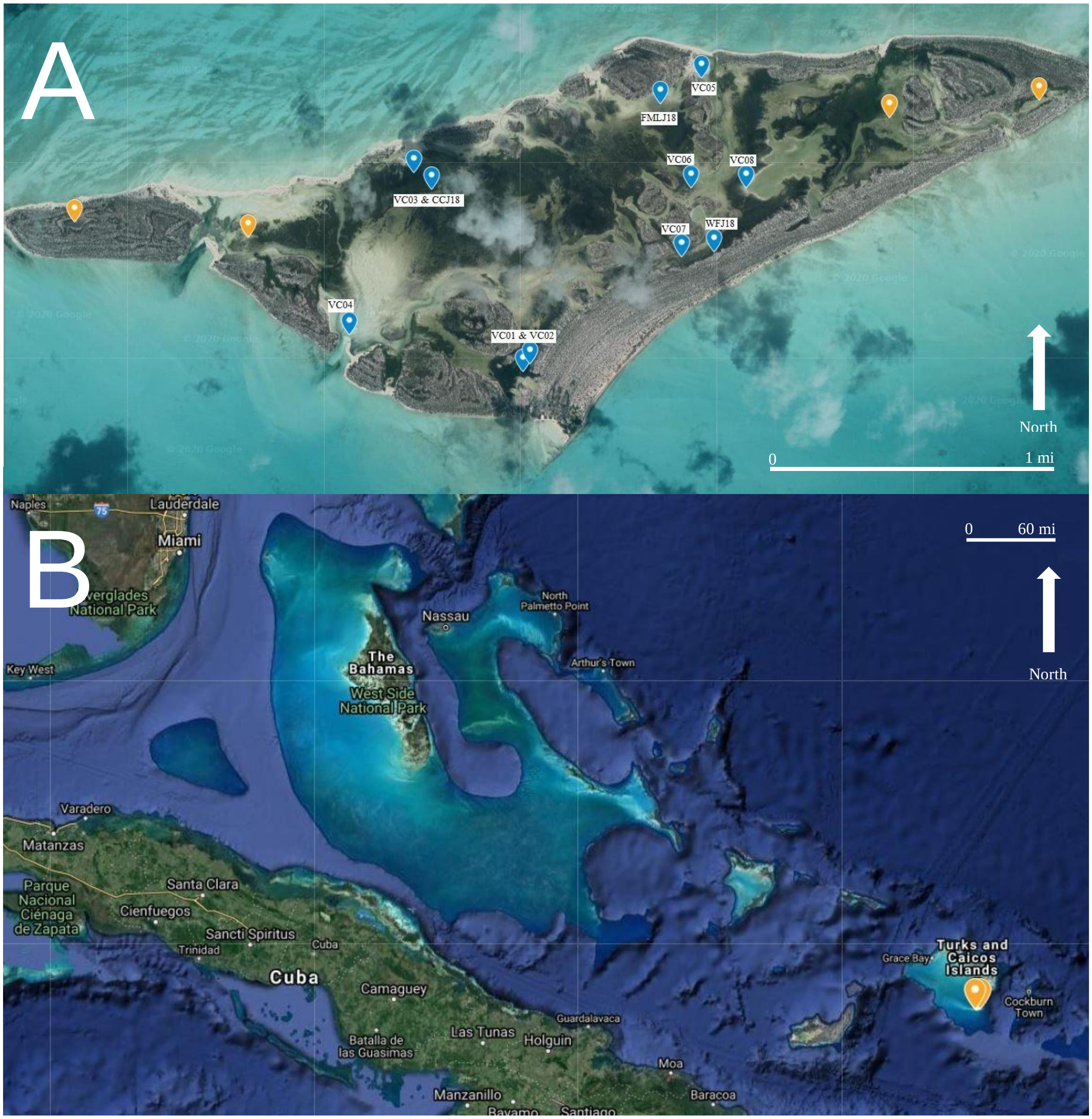
A
VC05
FMLJ18
VC06
VC08
VC03 & CCJ18
VC07
WFJ18
VC04
VC01 & VC02
North
0
1 mi
B
Naples
Lauderdale
Miami
verglades
National Park
Key West
0
60 mi
North
Nassau
North
Palmetto Point
Arthur's Town
The
Bahamas
West Side
National Park
Varadero
Matanzas
Parque
Nacional
Ciénaga
de Zapata
Santa Clara
Cienfuegos
Sancti Spiritus
Trinidad
Cuba
Cuba
Camaguey
Guardalavaca
Las Tunas
Holguin
Batalla de
las Guasimas
Moa
Manzanillo
Baracoa
Bayamo
Santiago
Turks and
Caicos
Islands
Grace Bay
Cockburn
Town

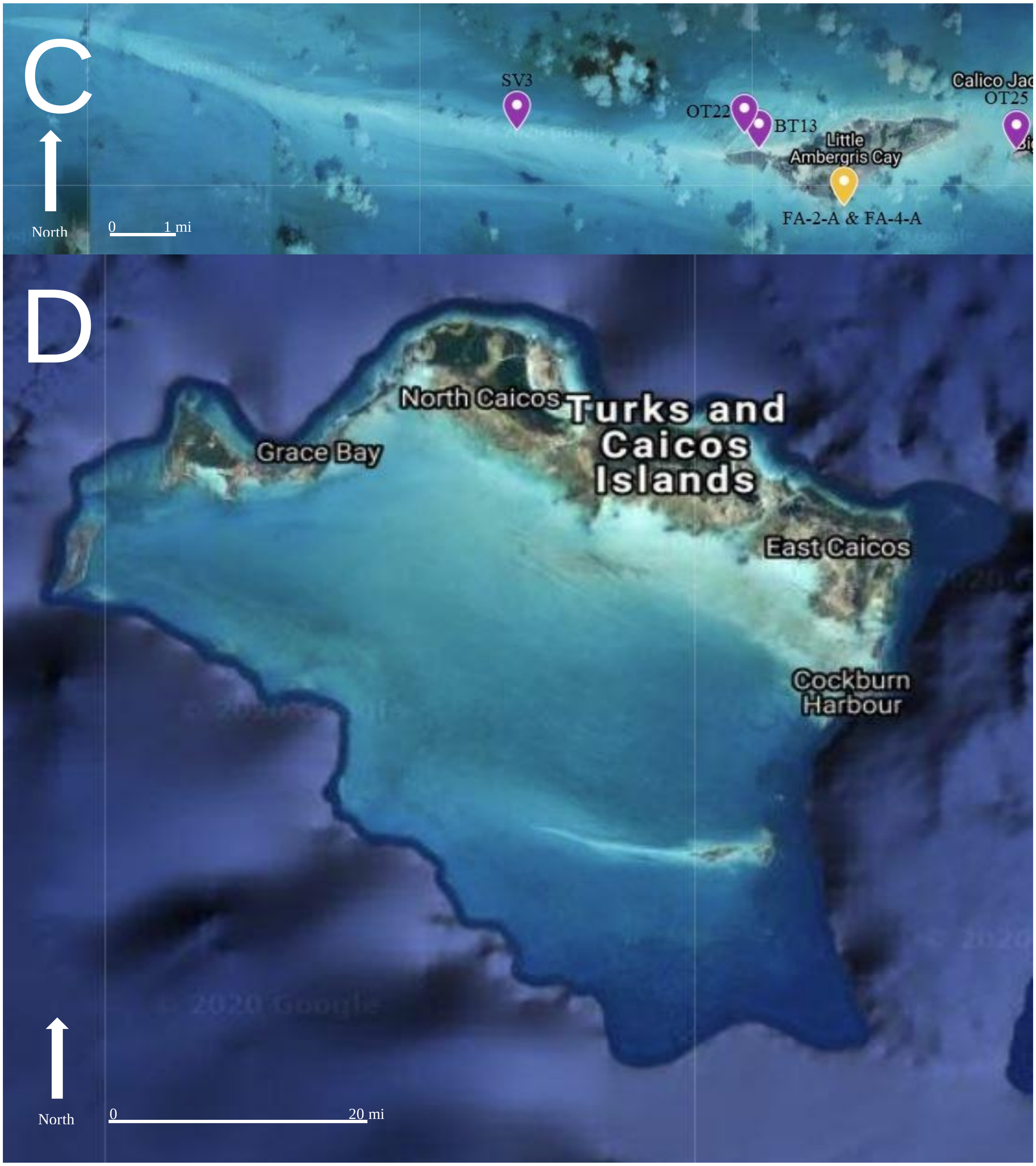

Figure 1:
A: A map of Little Ambergris Cay with associated core locations.
B: Little Ambergris Cay (Orange Pin) in relation to the broader geography of surrounding nations.
C: LAC in relation to the 20km westward shoal. Purple pins indicate cores of comparison facies discussed in Table 1. Yellow pin indicates additional bedrock radiocarbon data. The yellow pins of FA-2-A & FA-4-A lie at the southernmost corner of LAC.
D: The bottom image shows the Caicos Platform as a whole. LAC and its shoal are visible as the elongated island in the southern half of the map. Big Ambergris Cay lies to the east of LAC and is connected to LAC through the Intra-Cay shoal.

Little Ambergris Cay is located ~15km north of the Caicos platform southern margin, consisting of a ~7km shoreline and a ~20km linear ooid-shoal extending to the west of LAC (Figure 1.D). Easterly winds influence westward current, wave, and minor tide action (Trower et al., 2018 & Dravis and Wanless, 2008). LAC is almost entirely comprised of Holocene aged ooids, "concentrically coated sand-size grains composed of $CaCO_3$ minerals" (Wilkinson et al., 1985), which form in "shallow, current-agitated marine settings (Trower et al., 2018; Newell et al., 1960; Ball, 1967; Rankey and Reeder, 2011)." Ooids are known to form and grow by means of two different methods that are still researched today. The first method, after Trower et al. (2018), relates the high energy physiochemical relationship of sediment transport intertwined with unique seawater chemistry (that is high in carbonate concentration), thus allowing high rates of calcium carbonate precipitation. The second method, after Diaz et al. (2017), describes a low energy transport regime incorporated with microbial influence, allowing biotic activity to increase calcium carbonate precipitation rates. Both methods are accepted, however along the high energy environment of LAC, the transport induced formation and growth is most applicable. LAC's high concentration of ooids provide yet another reason as to why its individual formation does not follow modern platform island growth. Modern analogues (Florida and the Bahamas) typically accrete from photosynthetic carbonate production influence (such as corals), with minor ooid concentrations (Schlager, 2003). LAC provides a case study of island formation that appears to be dependent on a steady supply of ooids, with a unique absence of biotic influence.

The Caicos platform is strongly influenced by wind-wave processes, in contrast with other well-studied modern carbonate environments like Florida and the Bahamas, which are tidally dominated (Dravis and Wanless, 2008). The ooids of the Ambergris shoal to the east of LAC reflect the wind-wave influence, where Trower et al. (2018), through an analysis of radiocarbon ages of ooids, observed that westward migrating ooids become younger in age, and larger in size. This indicates that ooid growth is occurring through transport along the western shoal of LAC. Dravis and Wanless (2008) also determined that Big Ambergris Cay is the product of a preexisting high (>25m) Pleistocene island. Considering that the islands on the northern and eastern sides of the Caicos platform also reflect a Pleistocene reefal rim (Dravis and Wanless, 2008 & Kerans et al., 2019) (Figure 1.D), and that LAC is located on the interior of the Caicos Platform and is composed of Holocene aged bedrock (which developed on top of the existing Ambergris shoal) (Orzechowski et al., 2016), LAC could not have formed through the same mode of island development as the other Caicos islands. Rather, given the wind-wave dominant influence on LAC, and the interpreted eolianite ooid grainstone bedrock, a new facies model must be concluded to give insight into Caicos interior platform growth that is not a product of preexisting island or tide influence, but instead of wave and wind influenced processes.

Given these two observations of accumulation during sea level rise, and westerly ooid production, I will attempt to understand the depositional environment of LAC, and provide information that can further the research and understanding of carbonate platform development in similar global environments.

Before research was conducted, I developed hypotheses regarding the question of how an island forms during a period of sea level rise. I hypothesized that, in order for an island to form, sediment supply must have outpaced sea level rise (accommodation space). Trower et al. (2018), proposed a westward growth hypothesis of LAC, which I decided to test through facies development and stratigraphy. It is known that current and wind influence westward migration of sediment (Trower et al., 2018; Dravis and Wanless, 2008), and Big Ambergris Cay lies to the east of LAC and is older in age. Given this observation, I hypothesize that sediments from BAC are migrating to LAC where early lithification of ooid grainstones could have trapped incoming sediments. I therefore also developed an alternative hypothesis that Little Ambergris Cay accreted eastward, towards BAC, as a function of incoming sediment supply onto a pre-existing bedrock.

Three steps will be taken in testing these hypotheses (westward vs eastward accretion), by analyzing sediment sample characteristics from cores collected on the interior of LAC. Using point counting data (Figure 3), I am able to determine sediment composition within the VC03 core. Secondly, I used Matlab to analyze Camsizer data, and was able to determine characteristic grain size (D_{10}, D_{50}, D_{90}), mean roundness, and sorting for the other cores (VC01-VC08). By comparing the point counting data to the Camsizer data for VC03, I determined that the roundness, grain size and sorting parameters correlated to the interpreted grain composition. Because grain composition gives insight into sedimentary facies and depositional environment interpretations, I was able to use these parameters from Camsizer data to identify and interpret facies changes in the remaining cores. I used stereoscope microscopy to check that my interpretations of grain composition and facies changes via Camsizer data for the other cores were supported. The third and final step was to use both the point counting and Camsizer data, compared against a set of thin sections and Camsizer data, for samples that represented modern depositional environments to determine facies and environmental change over time on LAC.

Based on the conclusions that I draw in these three steps, using the parameters described above, I will test that the westward growth hypothesis of Little Ambergris Cay (Trower et al., 2018) is not supported by the data analyzed in this paper. Rather, based on the facies development of the VC cores and the comparison facies deposits of Table 1 & 2, I will attempt to support an eastward growth hypothesis of Little Ambergris Cay.

Materials and Methods:

Considering the recent changes due to COVID-19, most research was conducted over remote methods of analysis, using multiple programs to help determine parameters that would best reflect depositional environment.

Sediment Core and Sample Collection

I began work on a set of sediment samples collected from a variety of depths in eight sediment cores previously collected in 2017 and 2018 via vibracoring. The deepest cores worked on were VC03 and VC04, extending to a maximum of 220 and 230 cm, while the shallowest cores were VC02 and VC06, both extending to a maximum of 100cm. The shallowest depth collected within all the cores was 20cm. The increment sampling resolution was 20cm in each core. The cores were found in surrounding locations on the interior of Little Ambergris Cay as described in Figure 1.A.

Point Count Analysis Data

The first step was to conduct a point count for sediment composition using JMicrovision, an image analysis toolbox. Analyzing 11 thin sections of the loose sediment in VC03, at each successive depth (up to 220cm), I performed a 400-sample point count for each increment depth. Each depth displayed changes in ooid, peloid, grapestone, bivalve, gastropod, *Strombus Gigatus*, desiccated microbial mat, loose carbonate, and unidentifiable skeletal grain abundance. Figure 3 describes the interpreted point counting data as a percentage of the 400-point sample. The goal of performing this point count data was to get an understanding of grain composition, and how changes in concentrations of certain grains could provide a point of interest to begin interpreting aspects of the samples grain characteristics, like sorting, roundness, diameter, etc.

Grain Size and Shape Data

The next step was to analyze grain size and shape data, which had previously been measured via a Retsch Camsizer P4, from all the cores through a Matlab code that was able to process the D_{10}, D_{50}, D_{90}, mean roundness, mean sphericity, mean aspect ratio, roundness, and sorting. By running a code for the VC01-08 cores, an output file containing a graph of sediment distribution is produced, as well as a raw data file containing values that we can correlate to characteristics of interest (like sphericity, aspect ratio, diameter, etc.). These data allowed me to determine which parameters best described the point count data.

Roundness, grain diameter (D_{50}), and sorting will be used as parameters for comparison in this research.

Roundness is described by Wadell (1932) as:

$$Roundness = \frac{\sum_{i=1}^{n}\left(\frac{r_i}{R}\right)}{n}$$

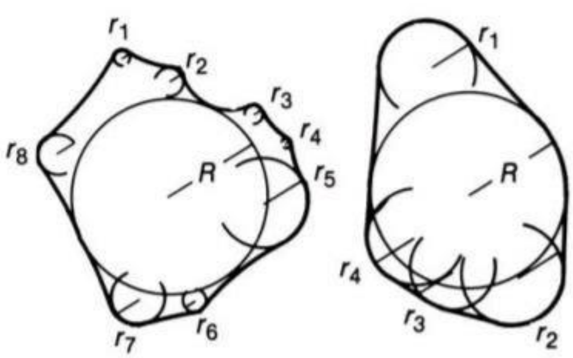

Figure A: Krumbein's (1940) photo depicting variables required in calculating roundness based on grain shape.

“Where r(i) is the radius of curvature of particle corners, R is the radius of the largest inscribed sphere, and n is the number of particle corners measured.”

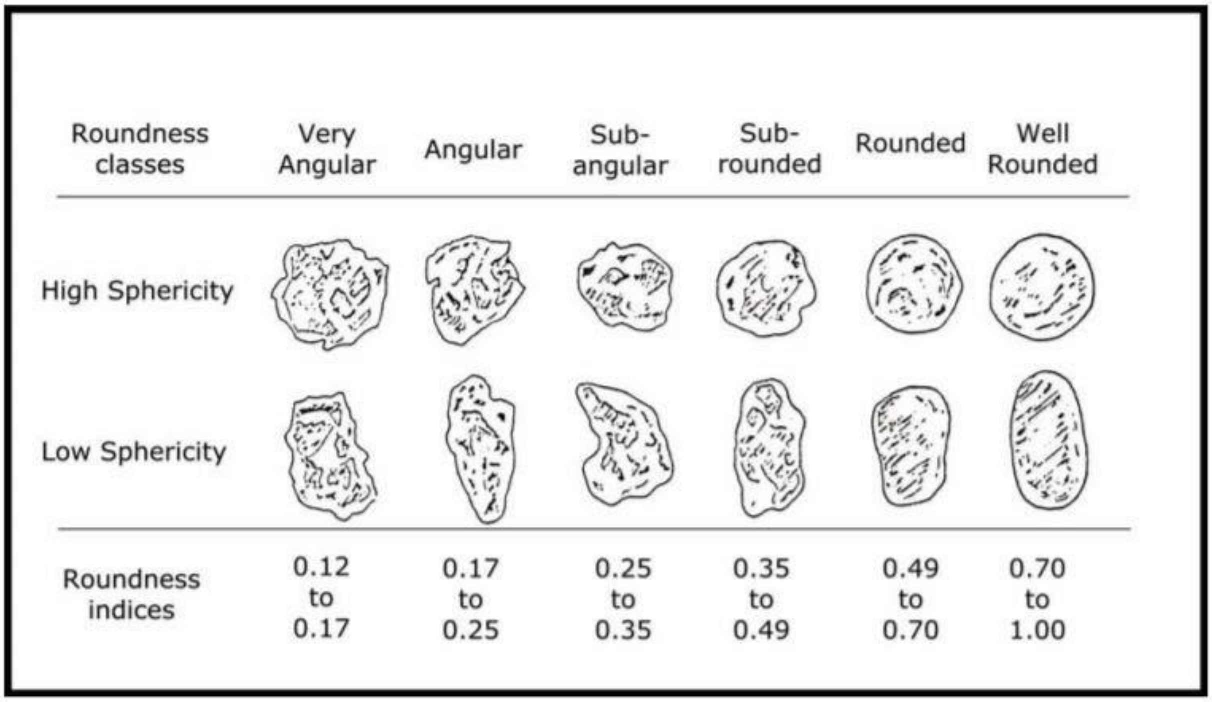

Figure B: Powers’ (1953) photo depicting physical representation of rounding and sphericity and their associated values.

D_{50}, or median diameter of the grain sample, is described as “Particle diameter representing the 50% cumulative percentile value (50% of the particles in the sediment sample are finer than the D_{50} grain size), in microns (USGS).” D_{50} can highly range in values depending on the environment of deposition, where a sample of extremely coarse grains display a high median diameter, and fine grains produce a low diameter.

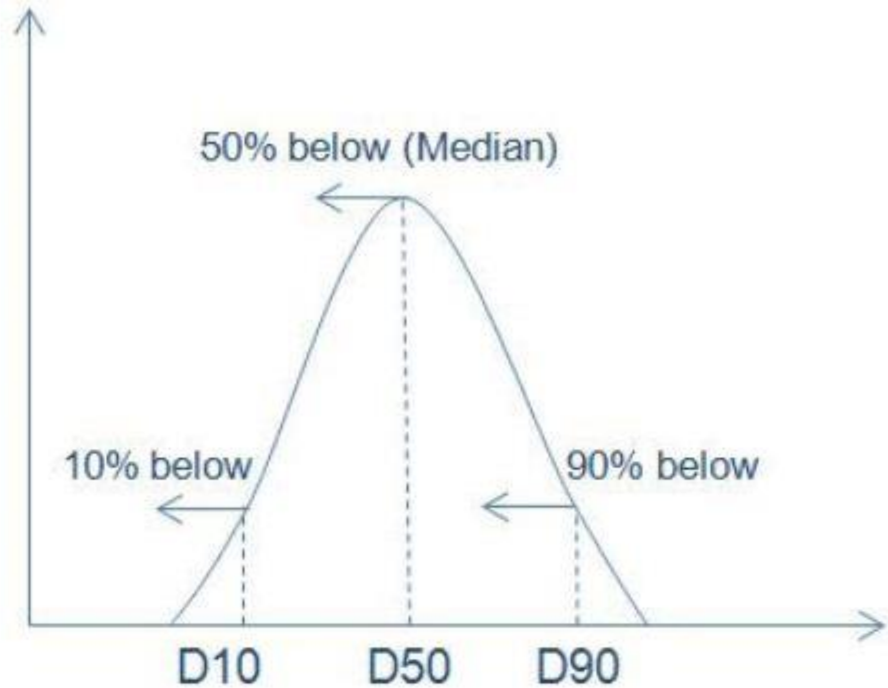

Figure C: Entegris (2020, *What is the Effect of Sample Size on Particle Size Distribution Measurements?*) photo depicting D_{10}, D_{50}, and D_{90} as a standard deviation plot representing how each parameter describes grain size. For example, 90% of the sample grains are of size finer than the D_{90} value.

De Mahiques (2016) describes sorting as "the degree of dispersion of a grain-size distribution around a central value (mean, median, or mode)." Folk and Ward (1957) introduced the widely accepted practice of using 68 % and 90 % of the median value to define sorting criteria: very well sorted, well sorted, moderately sorted, poorly sorted, and very poorly sorted.

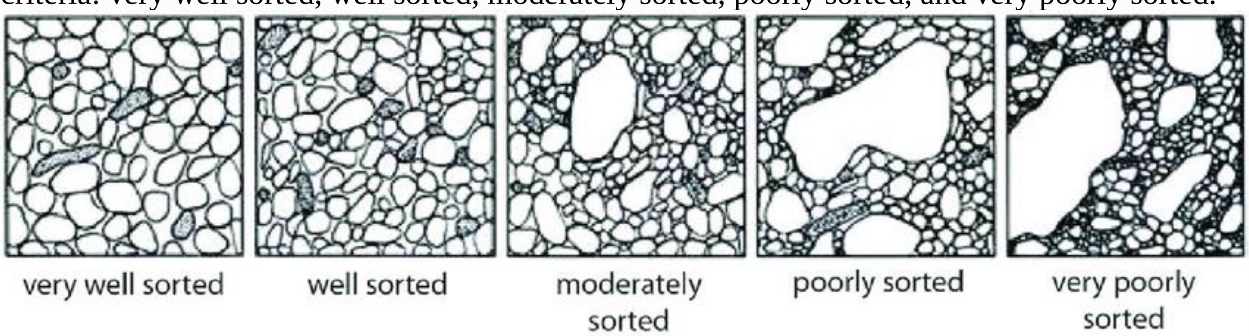

Figure D: Rian A. Dutch's (*ResearchGate*) photo offers a physical representation of the range of sorting.

Stereoscope Microscopy

Stereoscope microscopy was performed on the four samples described in Figure 4, 5 and 6. I examined the loose sediment VC samples under a series of different magnifications and lighting to best capture an idea of how the Camsizer data translated physically, since there were only thin sections prepared from one core (VC03). This imaging allowed me to qualitatively assess the abundance of ooids and skeletal grains, and confirm the Camsizer sorting, roundness, and diameter data.

Radiocarbon Data

Radiocarbon dating was performed on 11 samples (Figure 2 & FA-2-A and FA-4-A) via Accelerator Mass Spectrometer (AMS) at the Keck-Carbon Cycle AMS facility at UC Irvine and the NOSAMS facility at WHOI. With provided dates of rough sediment age analyzed by radiocarbon analysis, I applied a reservoir correction utilizing a free online software named "Calib Radiocarbon Calibration (Calib)" to the ages of three cores, following the approach described in Trower et al. (2018). "Calib" corrected uncertainty based on standard deviation and historic anomalies. By interpreting ages of sediment deposited on LAC, I was then able to begin correlating the depositional environments with respect to a rough time scale.

Facies Correlations to Modern Depositional Environments

Using sorting and roundness as a parameter for comparison, I ran the same Matlab code, as used for the VC's, for given modern depositional environment's thin section and Camsizer data that represented a shoal, intra-cay shoal, open platform, beach, and storm deposit facies (Trower et al., 2018; Jamison-Todd et al. 2020; Table 1). By collecting the sorting and roundness data for the representative environments, I was able to compare the previously processed sorting and roundness data of the VC cores and correlate each depth's values to the associated representative environments. This allowed me, along with the radiocarbon age of the given cores, to formulate an idea of how facies changed over time.

<u>Results</u>:

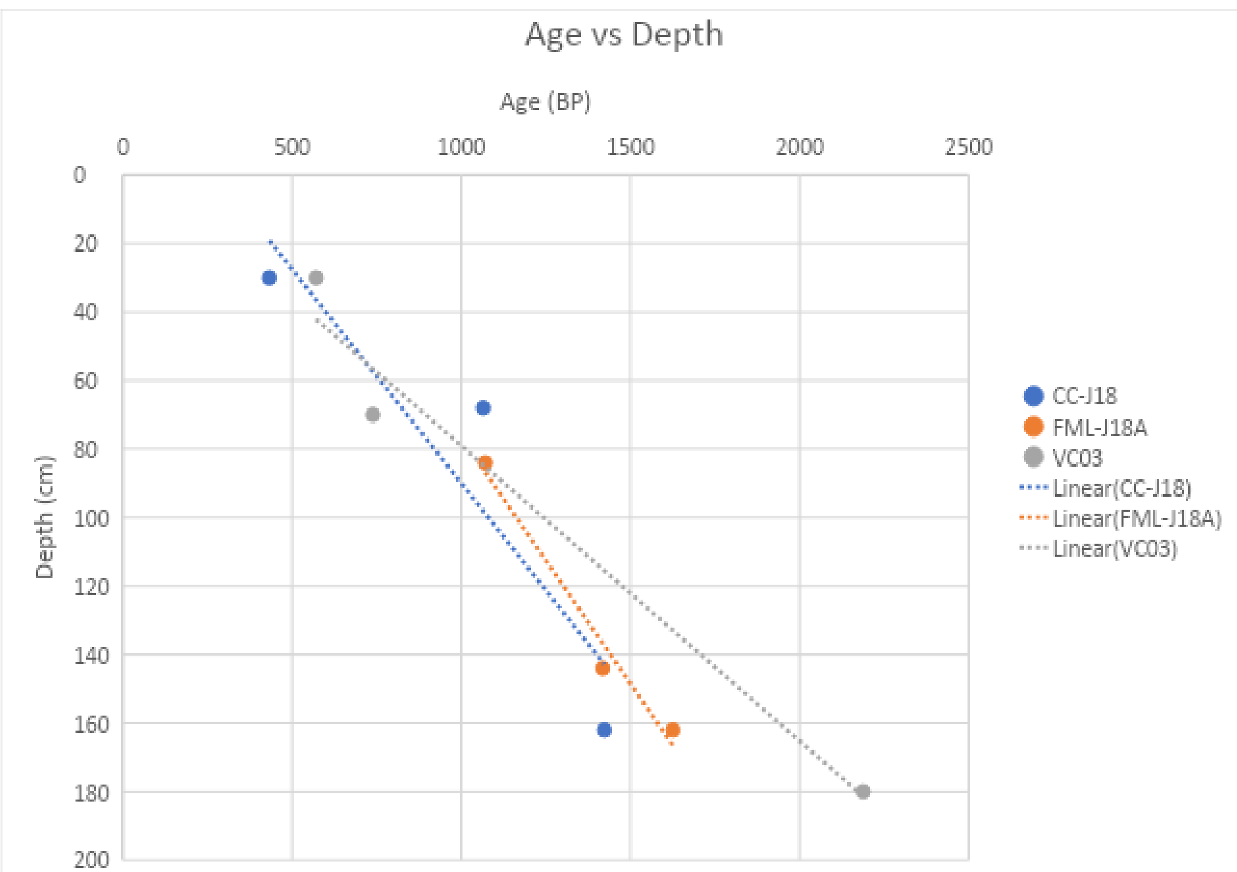

Figure 2: Corrected radiocarbon data for three cores collected on northern LAC.

The ages of the three cores (ranging from youngest to oldest) display similar trends vs. depth between each core. CC-J18 and VC03 are in similar positions on the northern side of LAC, while FML-J18A is located on the eastern side of LAC (Figure 1.A) Corrected radiocarbon age for exposed bedrock samples FA-2-A & FA-4-A (Figure 1.C) show ages of 5946BP & 5220BP. The bedrock has been interpreted as a cross-stratified eolianite ooid grainstone (Orzechowski et al. 2016).

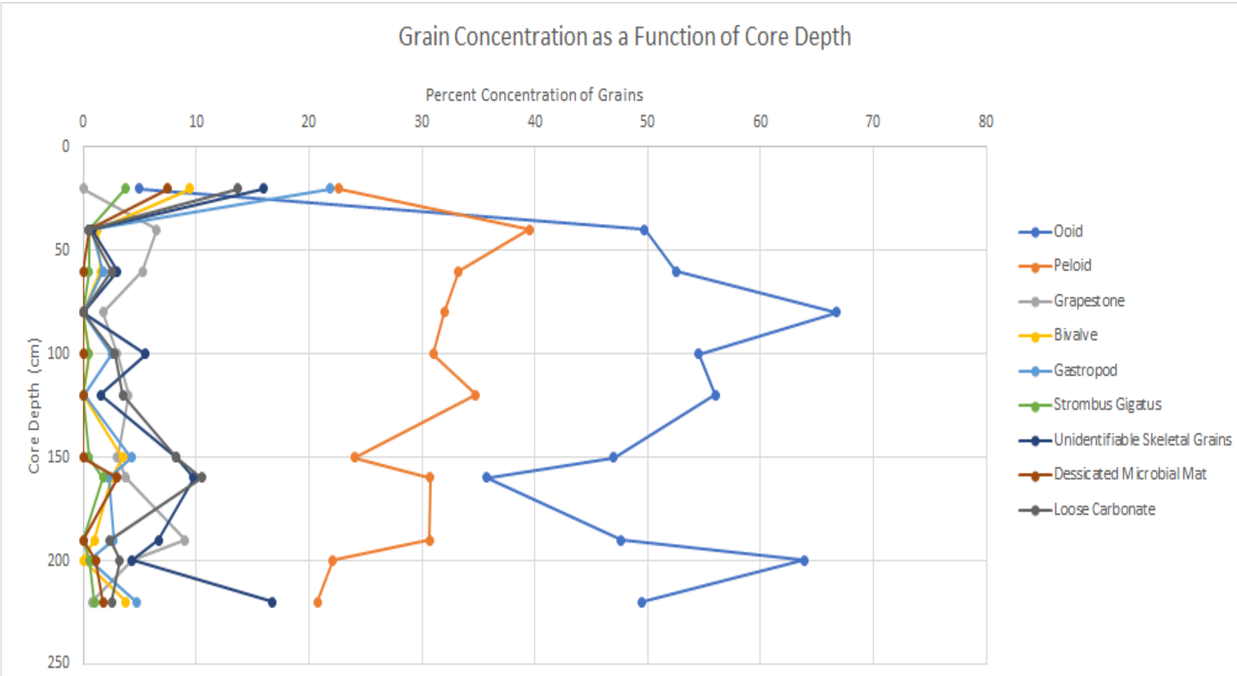

Figure 3: The scatter plot above shows sediment compositions a function of core depth.

The data was determined through a 400-sample point count for each depth in VC03. Trends imply that skeletal grains were abundant in the shallower and deeper sections of the core, and ooid abundance increased in the mid-core (60cm+) and decreased in the late-core (~150cm), followed by another period of increase (~180cm). Sediment composition provides key information into depositional environment and will be discussed in more specific analysis further in the discussion.

Each depth displayed offers three general trends: percent changes in ooid, peloid, and skeletal grain abundance. I determined that roundness, median diameter (D_{50}), and sorting, as provided through Camsizer analysis, best correlated with the changes in concentration of ooid and skeletal presence described in Figure 3, and should thus be interpreted for other cores of interest as described in Figures 4, 5 and 6.

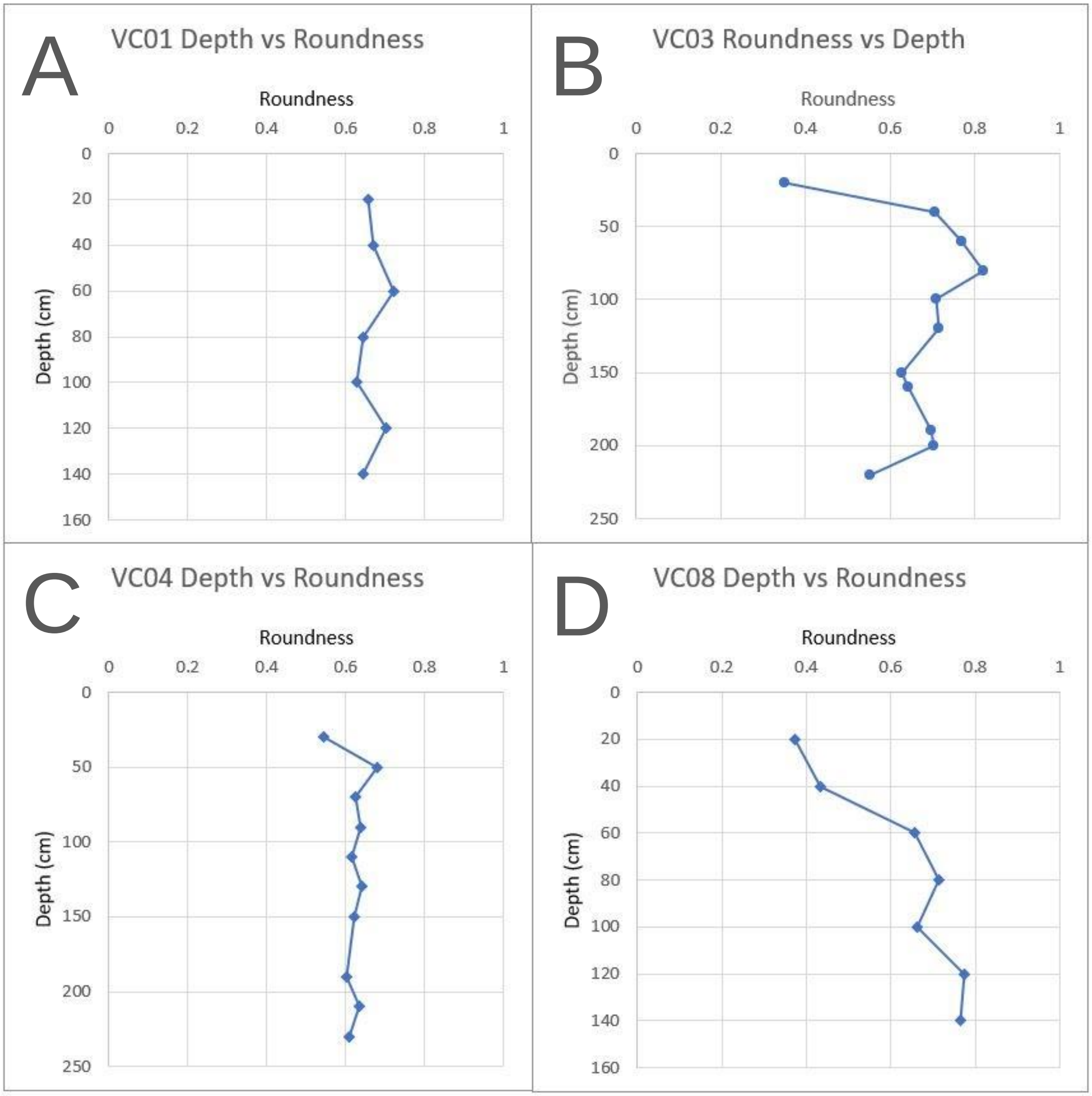

Figure 4: The photos above represent each core's depth compared against roundness. The higher the values, the higher the roundness.

Four cores were chosen to compare roundness, D_{50}, and sorting versus depth to serve as a proxy for ooid concentration. Each core is located within different cardinal direction points around LAC (Figure 1.A) to give an interpretation of ooid concentrations based on differing locations.

The maximum roundness described in Figure 4.B is 0.81 in VC03, while the minimum value is 0.38 in VC08. Each core shows different patterns vs. depth, where VC08 increases with depth, and VC03 initially increases, but gradually decreases following 100cm. VC04 and VC01 remain relatively constant throughout their entire section.

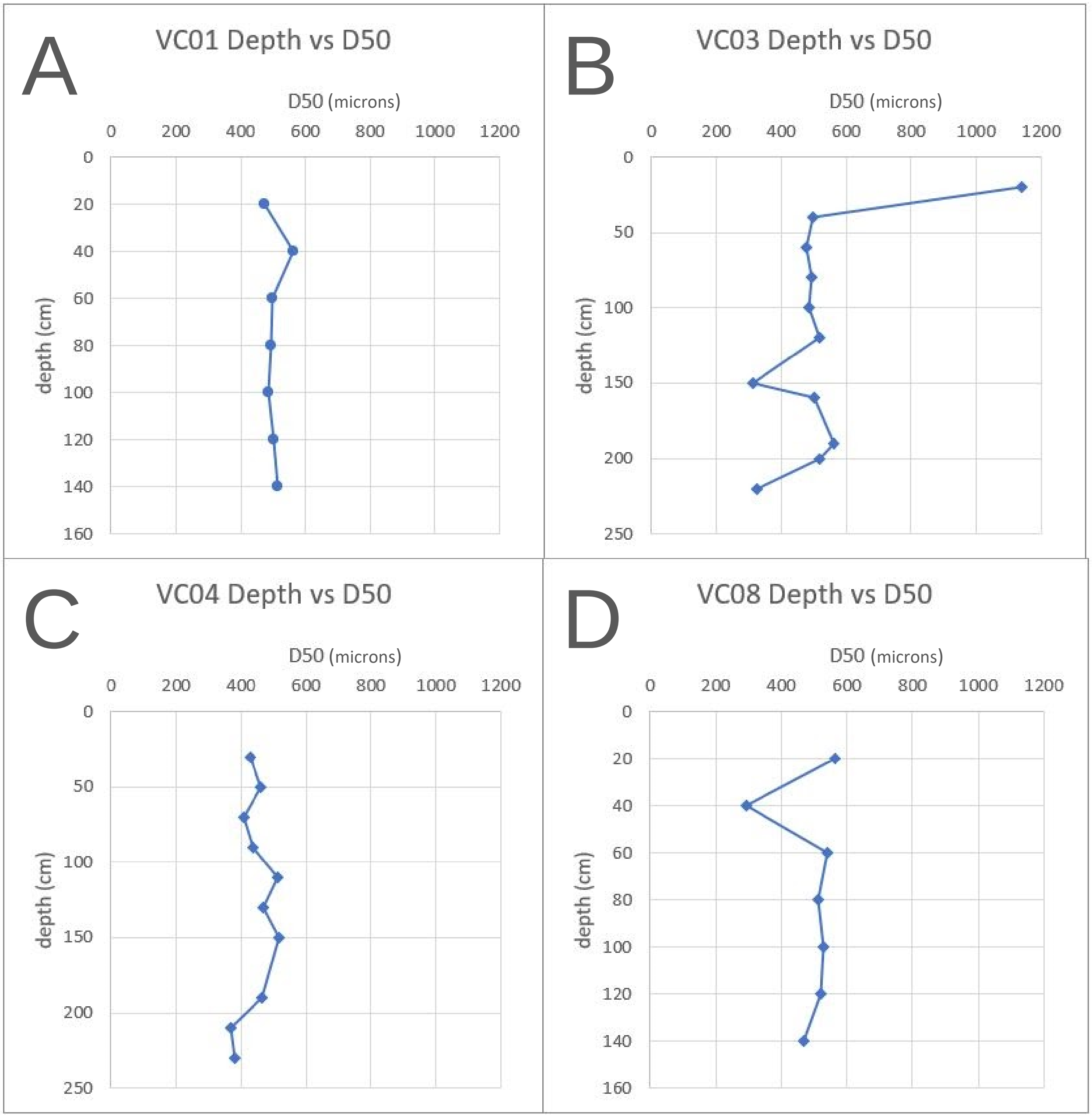

Figure 5: The photos above represent each core's depth compared against $D_{50,}$ or the median diameter. Units of D_{50} are in microns.

The maximum median diameter within the described cores is just <1200m in VC03. The minimum median diameter is ~300m in VC08. Once again, VC04 and VC01 display relatively consistent values throughout their section. Median diameter gives an interpretation of overall grain size, where consistent values of D_{50} represent consistent grain composition.

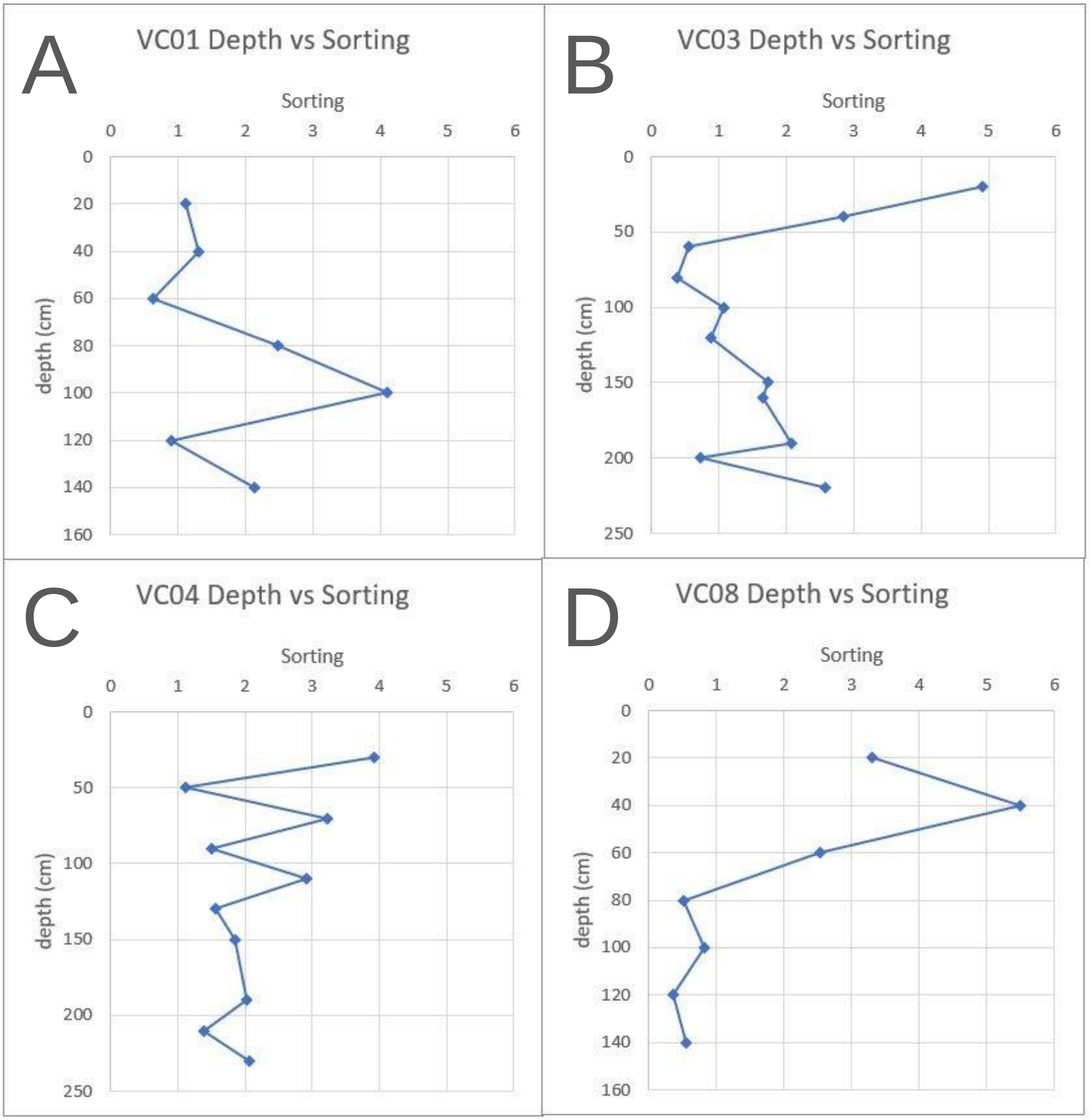

Figure 6: The figures above represent each core's depth compared against sorting. Higher numbers reflect poorer sorting.

The lowest degree of sorting is described in VC08 at ~5.5. The best degree of sorting is also within VC08 at 0.35 at 80cm depth. VC03 also exhibits a high degree of sorting at 0.38 at 60cm depth. Sorting provides an interpretation of grain presence, where the best degrees of sorting for LAC are consisting of dominantly ooids, and the lower degrees are a large mix of skeletal grains with ooids.

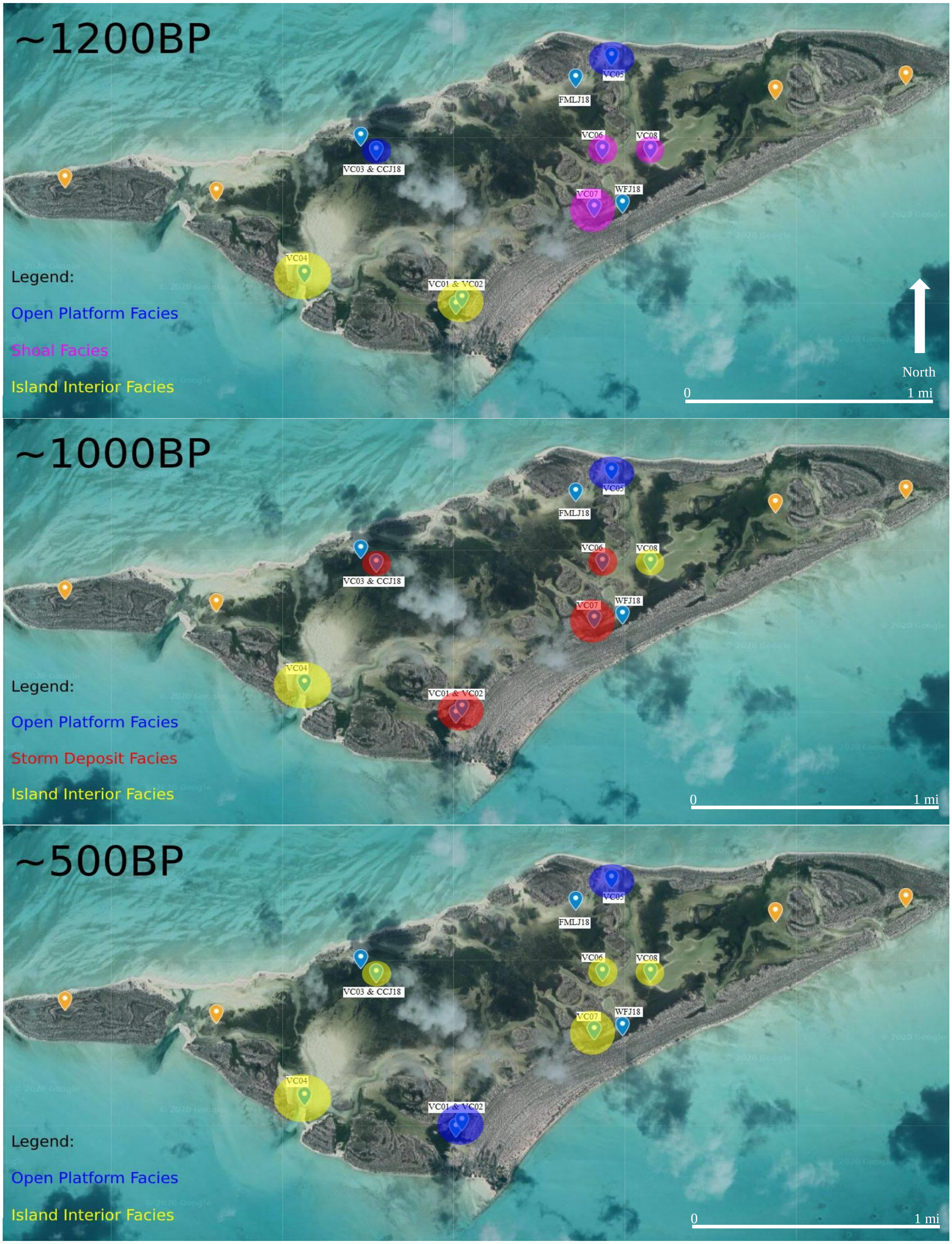

Figure 7:
The three photographs above show the interpretation of the succession of depositional facies through time based on the radiocarbon ooid data collected (Figure 2).

Facies were interpreted based on provided proxy facies for shoal, open platform, interior island, and storm deposit environments that are shown in Table 1. Interpretation of the depositional succession indicates that growth of LAC occurred towards the east, with minor fluctuations in open platform and shoal presence.

Proxy	Roundness	Sorting	Interpreted Depositional Environment
BT13	0.9284	0.629063	Beach/Shoreface
OT22	0.6357	1.338645	Open Platform
OT25	0.7115	0.816479	Intra-Cay Shoal
SV03	0.8173332	0.477957	Shoal
WFJ18	0.7602646	0.56311	Storm Deposit

Table 1: Given proxies for modern representative depositional environments and their associated roundness and sorting values.

Core	<30 cm	60-70 cm	95-110 cm
VC01	Open Platform	Storm Deposit	Island Interior
VC02	Open Platform	Storm Deposit	Open Platform
VC03	Island Interior	Storm Deposit	Open Platform
VC04	Island Interior	Island Interior	Island Interior
VC05	Open Platform	Open Platform	Open Platform
VC06	Island Interior	Storm Deposit	Shoal
VC07	Island Interior	Storm Deposit	Intra-Cay Shoal
VC08	Island Interior	Island Interior	Intra-Cay Shoal

Table 2: VC core depositional environments for three depths analyzed based on representative environmental sorting and roundness values in Table 1.

Facies interpretations were concluded by comparison against given depositional environment's roundness and sorting data. VC roundness and sorting were measured through Matlab Camsizer analysis and compared against the representative facies in Trower et al. (2018). Table 2 shows that a series of high to low energy shifts occurred across LAC and allowed general eastward succession from the intra-cay shoal to island interior facies.

Discussion:

Supporting Eastward Accumulation of LAC

VC03:
This section will look at how VC03 developed over time as a means of supporting eastward LAC accumulation.

VC03 at ~95cm depth most closely resembles the Open Platform Facies based on Figure 4.B's roundness, Figure 5.B's median diameter, Figure 6.B's sorting, and Table 1's comparison values, which correspond to a relatively high abundance of skeletal grains in the presence of medial degrees of ooid abundance, based on point count data (Figure 3).

VC03 at ~70cm depth most closely resembles the Storm Deposit Facies based on Figure 4.B's roundness, Figure 5.B's median diameter, Figure 6.B's sorting, and Table 1's comparison values, which correspond to high abundance of ooids (~68%) based on point count data (Figure 3).

VC03 at 20cm depth most closely resembles the Island Interior Facies based on Figure 4.B's roundness, Figure 5.B's median diameter, Figure 6.B's sorting, and Table 1's comparison values, which correspond to extremely low quantities of ooid abundance, and high skeletal grain presence, as noted in Figure 3's point count data.

There was not a given proxy for Island Interior Facies, and it was thus deduced that the commonly shallow depth/upper core recurring facies of low roundness and extremely poor sorting was the result of a low energy environment that contained an abundance of skeletal grains and lower ooid concentrations - most probably indicative of the interior of an island where little energy influence from the surrounding marine environment reduced ooid influx and allowed deposition of in-situ biological presence. Based on the sorting values in Figure 6.B alone, it can be concluded that VC03 at 20-30cm depth most closely resembles an Island Interior Facies.

*It should also be noted that VC03 exhibits the highest D_{50} value compared to the following three cores. It can be seen in the stereoscope images of VC03 below, that the 20cm depth of VC03 shows extremely high skeletal presence and uniquely larger grains.

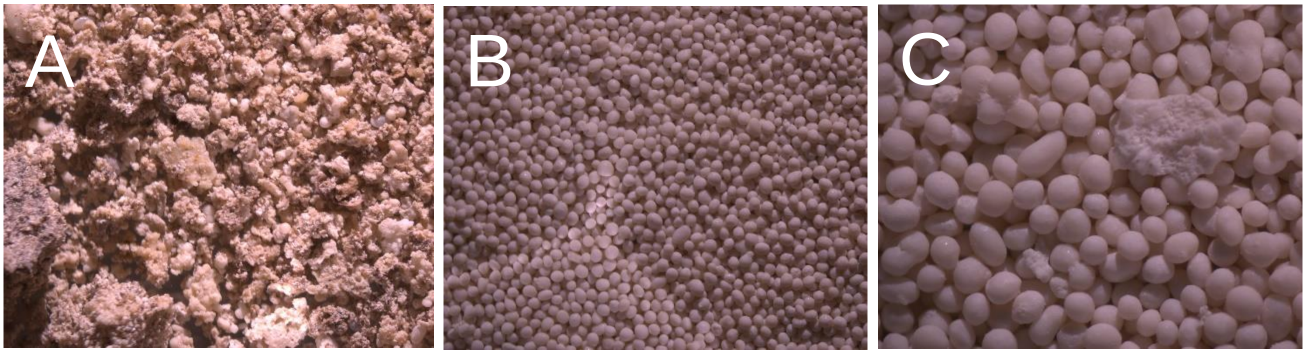

Figure 8: VC03 stereoscope images and their interpreted depositional environment: A = 20cm, Island Interior; B = 80cm, Storm Deposit; C = 100cm, Open Platform

VC03's point counting data (Figure 3) provided me an opportunity to determine sediment composition in one core and allowed me to visualize what parameters correlated with my interpreted results based on Figures 4, 5 and 6. By comparing the data of roundness (where high values correlate to high ooid abundance, and low values correlate to high skeletal abundance), D_{50} (where high values correlate to high skeletal abundance, and medial values correlate to high ooid abundance), and sorting (where low values correlates to high ooid abundance, and high values correlate to high skeletal abundance) of VC03, I was able to confirm that my point counting grain concentration data reflected the Matlab Camsizer analysis, and thus decided to use the three mentioned parameters as means of interpreting three other cores of interest: VC01, VC04, and VC08. By comparing cores that are in different geographical positions, and have exhibited differing trends in roundness, D_{50}, and sorting, we are able to confidently analyze island facies development.

	Roundness	Sorting		
VC03	0.64144117	1.643367	Open Platform	160cm (~1900BP)
	0.70326614	0.703266	Intra-Cay Shoal	200cm (~2400BP)

Table 3: VC03 roundness and sorting data for depths greater than 100cm and their interpreted depositional environments with rough ages

Because several cores only reached to 100cm depth, roundness and sorting data as a means of comparing facies was capped at 100cm. Some cores were able to provide roundness and sorting data for deeper sections, with VC03 being one of them. VC03's deeper data shows that the shoal facies may once have surrounded the majority of LAC's area, and eventually transitioned to the open platform as visible in Figure 7 at ~1200BP. Considering that the Intra-Cay Shoal is present as the earliest facies recognized for VC03, and also considering that LAC is argued to have initially formed on top of the shoal extending off BAC (Dravis and Wanless, 2008 & Figure 1.D), eastward accumulation is thus assumed, and will be discussed in the following sections.

All of the above data supports VC03's depositional settings as described in Figure 7.

Camsizer Data for Cores Displaying Variable Trends

In this section, I will be analyzing three other cores that, based on their Camsizer outputs, displayed differing comparison trends. I will argue that each of these core's roundness, median diameter (D_{50}), and sorting data, along with stereoscope imaging, support the facies development as described in Figure 7.

VC01:

At 20-30cm depth, based on Figure 4.A's roundness, Figure 5.A's median diameter, and Figure 6.A's sorting, VC01's shallowest depth most closely resembles the open platform facies (Figure 7 & Table 1).

At 60-70cm depth, based on Figure 4.A's roundness, Figure 5.A's median diameter, and Figure 6.A's sorting, VC01's mid core most closely resembles the storm deposit facies (Figure 7 & Table 1).

At 95-110cm depth, based on Figure 4.A's roundness, Figure 5.A's median diameter, and Figure 6.A's sorting, VC01's late core most closely resembles the island interior facies (Figure 7 & Table 1).

The stereoscope images below depict VC01's interpreted depositional environments at incremental depths.

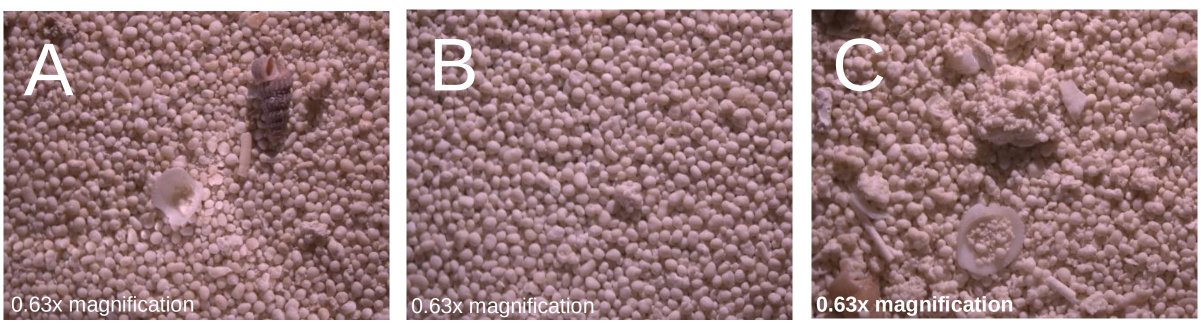

Figure 9: VC01 stereoscope images and their interpreted depositional environment: A = 20cm, Open Platform; B = 60cm, Storm Deposit; C = 100cm, Island Interior

VC08 in Figure 4:

At 20-30cm depth, based on Figure 4.D's roundness, Figure 5.D's median diameter, and Figure 6.D's sorting, VC08's shallowest depth most closely resembles the island interior facies (Figure 7 & Table 1).

At 60-70cm depth, based on Figure 4.D's roundness, Figure 5.D's median diameter, and Figure 6.D's sorting, VC08's mid core most closely resembles the island interior facies (Figure 7 & Table 1)

At 95-110cm depth, based on Figure 4.D's roundness, Figure 5.D's median diameter, and Figure 6.D's sorting, VC08's deep core most closely resembles the Intra-Cay shoal (Figure 7 & Table 1).

While the island interior facies for VC08 range from 0.3 roundness to 0.6 (a relatively large range for correlating), the sorting is the main feature to consider, as high skeletal abundance indicates a low energy environment where little influence from incoming wind-wave energy allows biological presence. The stereoscope images below depict VC08's interpreted depositional environments at incremental depths.

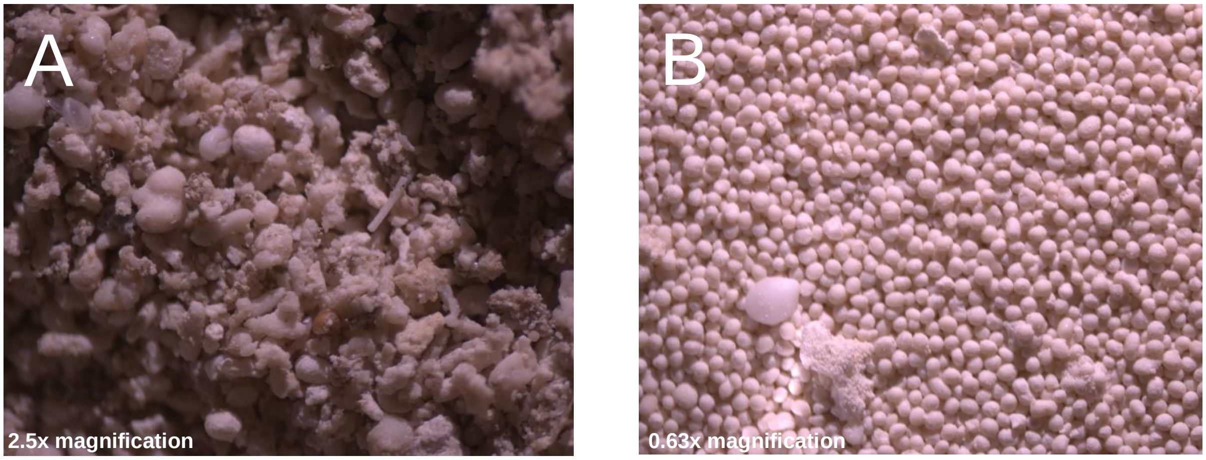

Figure 10: VC08 stereoscope images and their interpreted depositional environment*:* A = 20cm, Island Interior; B = 100cm, Intra-Cay Shoal

VC04 in Figure 4:

At 20-30cm depth, based on Figure 4.C's roundness, Figure 5.C's median diameter, and Figure 6.C's sorting, VC04's shallowest depth most closely resembles the island interior facies (Figure 7 & Table 1).

At 50-70cm depth, based on Figure 4.C's roundness, Figure 5.C's median diameter, and Figure 6.C's sorting, VC04's mid core most closely resembles the island interior facies (Figure 7 & Table 1).

At 95-110cm depth, based on Figure 4.C's roundness, Figure 5.C's median diameter, and Figure 6.C's sorting, VC04's deep core most closely resembles the island interior facies (Figure 7 & Table 1).

One interesting facet of VC04 is the relatively consistent high roundness that is associated with its location in the island interior facies. The poor sorting allows indication that the location has remained island interior throughout its Holocene history. However, compared to the other cores that exhibit island interior facies in the shallow depths (20-30cm) (VC03, VC06, VC07 and VC08), VC04 is the only core to see a roundness not within the range of 0.34-0.47. In fact, VC04 is the only core to exhibit Island Interior Facies throughout the entire interpreted time scale (Figure 7), as well as consistently exhibit roundness within the 0.54-0.62 range.

This could be due to VC04's geographic location, as well as being a core near the interpreted starting point of island eastward accretion. Note that VC04 lies just above a point where a channel from the marine environment is in contact with the island interior (Figure 1.A). It is possible that this channel is able to supply a steady amount of ooids to VC04's location, accounting for the specifically higher roundness observed.

Based on Figure 7's succession of facies, VC04 is the pseudo-starting point for eastward island accretion. Knowing that LAC provides a unique depositional analogue because it does not follow the most obvious island growth models (its outpacing of SLR is not consistent with common methods of platform growth), and because of its uniquely dominant ooidic composition, VC04 thus provides a starting line in determining a new method of platform interior island development. The stereoscope images below depict VC04's interpreted depositional environments at incremental depths.

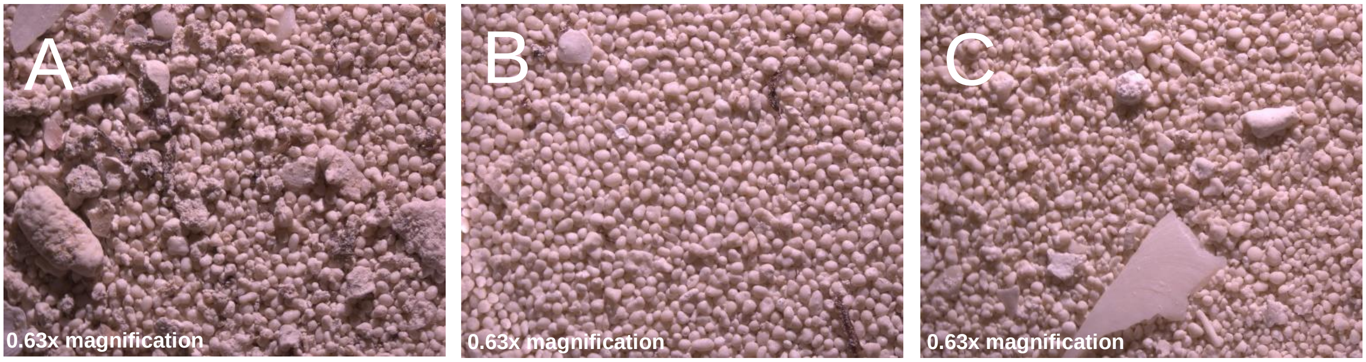

Figure 11: VC04 stereoscope images and their interpreted depositional environment: A = 30cm, Island Interior; B = 50cm, Island Interior; C = 190cm, Island Interior?
Note that the stereoscope image on the right is regarding a much greater depth than what is discussed above. However, the high amount of skeletals indicates that even at such depth, the island interior facies still seem feasible. Also, worthwhile to note is the high concentrations of ooids in each photo, mimicking the uniquely high roundness found in VC04's Island Interior facies as discussed above.

The bedrock is of considerably older age than any other taken samples, where FA-2-A and FA-4-A are of ages 5946BP & 5220BP, respectively, and the loose sediment core ages do not exceed ~2300BP (Figure 2). Thus, the south-west corner of LAC gives us our launching point along with VC04 as to where LAC just may have started accreting. Considering how VC01 and VC02 lie closer to the given bedrock (Figure 1.C) than VC04, it is questionable as to why VC01 and VC02 change to an Open Platform facies in the early Holocene (~500BP) rather than remain Island Interior, as VC04 exhibits. This could be due to recent geographic changes of LAC, as the form of the island, and its subsequent curved-southern beach allows for a higher influx of ooids, and lowers the ability for presence of biological activity (thus producing higher roundness and better sorting) in VC01 & VC02's location (Figure 1.A & 5). This anomaly could also be due to a modern change in depositional environment but cannot be supported by the research done in this paper. It is recommended that further research be conducted on current wave-energy flux on the southern and south-western sides of LAC.

By looking at the individual roundness, grain size, and sorting data for the four cores mentioned above, I am able to confidently compare their statistics against the representative samples' Camsizer data (Table 1), which represent modern depositional environments. This allows me to interpret how LAC's environment changed with depth, and thus assert that all of the above data supports VC01's, VC04's, and VC08's depositional settings as described in Figure 7.

Developing a Facies Model

Schlager (2003) discussed three modes of carbonate facies development, the T, C and M factories. T represents a tropical water development, where carbonate accretion primarily occurs in shallow waters and typically (but not always) produces flat-topped or rimmed platforms. The C factory describes cool water environments, where carbonate accretion occurs across a broader range of water depths. The M factory represents "mud-mound" development, which is biologically induced, rather than biologically controlled (as the T and C factories are). The Caicos Platform is most similar to the classic T factory, as the interior of the platform only reaches depths of up to ~20m, (but averages ~4m along shoals and beaches, Dravis and Wanless, 2008; Harris et al., 2008) and is observed to have little to no barrier reef influence (micrite is not greatly observable in thin section, nor in Matlab analysis of grain composition (Figure 3)). Thus, after Schlager (2003) and Wilson (1975), we can examine the widely accepted facies models of rimmed platforms based on the Florida and Bahama analogues. It should be noted that, along with the theme of this research, that the Caicos Platform differs strongly from the Florida and Bahama models. The Caicos platform is wind-wave influenced, not tidal. The Caicos Platform also clearly indicates that facies patterns are primarily related to ooid shoals rather than reefs. Nonetheless, Schlager's facies models allow us to piece together portions of a depositional environment that replicate energy influence, while we can conclude lithologic composition based on the data provided for LAC (Figure 2).

To compare environments, we should assess LAC's geographic and topographic setting. Considering the prior existence of the Ambergris shoal that extends from BAC to the eastern edge of LAC, we know that accumulation of ooid sediments occurred atop this shoal. This would indicate that LAC's topography was relatively flat and shallow. Geographically speaking, LAC is located within the interior platform. Considering both the low-relief topography and interior location, we can analyze facies models described by Schlager (2003), and place LAC within the "sand shoals," "platform interior normal marine" or "platform interior restricted" facies. "Sand shoals" are characterized by "Elongate[d] shoals and tidal bars, sometimes with eolianite islands; above fair-weather wave base and within the euphotic zone." "Platform interior" refers to a setting of "Flat platform top within euphotic zone and normally above fair-weather wave base." The "interior restricted" varies from the "normal marine" in that it has less connection to open sea influences, and thus sees higher lime-mud concentrations. Based on these definitions alone, it appears the "sand shoal" facies are the obvious contender for a replicate environment of LAC, even directly citing eolian islands. Considering this placement, let us then consider the energy environment of the "sand shoal" in relation to the rimmed platform overall. The most distinctive component of the "sand shoal" facies that Schlager portrays in his model is the well-preserved cross bedding. This would indicate that traction-transport plays a large role in accumulation of the "sand shoal" and can also be referenced in LAC's cross bedded bedrock grainstone, and Dravis and Wanless's ripple-laminated ooids.

Given the above information, a new facies model can be developed for LAC. Ooid growth is supported by westward wind-wave transport on the interior of the Caicos Platform (Trower et al., 2018). In a setting of preexisting shoal, eolianite formation clearly has an influence on accumulation of sediment, accompanied by strong influx of ooid grains from wind, waves, and storm deposits. Thus, a new facies model, one characterized by dominant ooid lithology and some skeletal presence can be concluded as follows:

Where? Platform Interior, along preexisting shoals/bars and parallel to wind-current paths

What? Dominantly ooid grains, with medium to high pellet/peloid content. Biota include shallow-water marine organisms such as gastropods, bivalves, and *Strombus Gigatus*

How? Wave-wind influence, crossbedding observed, eolianite formations possible

Overall Analogue: modern ability to accrete past a rising sea level is dependent on wind-wave influenced accretion of abundant material (in this case, ooids) among a pre-existing feature not consisting of bedrock, reef, or in-situ biology, but rather loose sediment features such as shoals, beaches or bars. Basically, sediment accumulation can outpace sea level rise; regarding early sedimentary learning concepts, **sediment supply is greater than accommodation space**.

Regarding the question of why LAC accumulates in the position it does (~3 miles off of BAC), instead of accreting off the western edge of BAC, I have formulated three hypotheses that could explain such formation.

1. BAC poses as a large geographic "block" for current and wind-wave influence coming in from the east. This "block" forces wave refraction off the northern and southern edges of BAC. It is possible that the two refractions combine at the ~3 miles mark where the initial bedrock could have lithified, thus allowing sediment supply to be particularly higher at this specific location, and in turn allowing eolianite processes or cement compaction processes to allow an early lithification.
2. Patch reefs are visible and have been observed around the entirety of the Caicos Platform (Dravis and Wanless, 2008). It is possible that a singular patch reef was/is in-situ at the ~3-mile point west of BAC. It is possible that the westward migrating ooids were able to be trapped in this patch reef, and in turn allow sediment accumulation to form an early lithification to surpass sea level rise.
3. Knowing that ooids are increasing in size as they transport west (Trower et al., 2018), it could be possible that the Intra-Cay shoal grew westward enough to sufficiently surpass water depth. In other words, it could be possible that the westward growth of ooids along the BAC shoal grew to high enough size in high enough concentrations that they were able to succeed sea level, and thus allow an early lithification along with eolianite processes.
    - Microbial mat influence has the potential to affect each of the above listed scenarios. While in-situ biology has not proved to be a leading cause of LAC island accumulation based on the research provided in this paper, it should be noted that microbial mats greatly increase the ability for sediment entrapment, and even minor presence of microbial mats could help support accumulation of incoming ooid sediments.

Future Directions

Unfortunately, based on the research concluded in this thesis, a fully supported working argument for the highly ooidic environment of the Caicos Platform cannot be reached, nor can the specific reason for development of LAC ~3 miles west of BAC. However, I propose that research be conducted on a series of processes within the Intra-Cay shoal and LAC. Based on the above hypotheses, the direction and energy relationship of refraction off BAC should be considered in how exactly the wave energy may influence the combination or direction of ooid sediment transport. Considering that the patch reef hypothesized may no longer be easily observed or studied, I would encourage research into the other observed patch reefs on the Caicos platform, and how ooid accumulation rates on these reefs correspond to sea level rise (AKA an accumulation rate vs. time) as well as energy influence (do faster or slower currents indicate lower or higher sedimentation rates?). Finally, research on the westward development of ooid growth has shown that west of LAC, a 1 mm/yr. growth rate (Trower et al., 2018) is observed. This does not indicate that ooid growth could surpass current sea level rise rates. However, LAC is on only one interior section of the Caicos Platform, and I would encourage other ooid growth rates to be researched on other shoal sections of the Caicos Platform, as well as research into the seawater chemistry and climatic controls that may govern uniquely high ooid precipitation. Further, the scope of this study did not cover late Holocene or early Pleistocene shoal/ooid development, but rather focused on the resulting processes revolving around a pre-existing ooid shoal. More research is needed into specific environments that display similar morphological shoal and seawater chemistry characteristics, to identify how wave, reef, and/or growth hypotheses interplay between the dynamic of shoal morphology and sediment accumulation.

Conclusion:

Building the Overall Picture of Little Ambergris Cay Formation

1. The Ambergris Shoal (Intra-Cay Shoal), extending a total of ~2.2km west (reaching the modern LAC shoreline) of BAC, of age greater than 6000BP, develops due to easterly wind-wave action and the prior abundance of ooid grains.
2. An abundant supply of ooids are continuously transported from BAC to the west, accumulating and extending along the Intra-Cay shoal.
3. Sediment supply outpaces accommodation space following the eolianite influence of LAC ooid bedrock lithification ~5946BP. Possible reasons for sediment supply to accumulate past the subsurface and lithify could be due to wave refraction induced sediment accumulation, patch reef presence and subsequent sediment accumulation, or transport induced ooid growth resulting in carbonate sediment growth surpassing sea level rise.
4. Westward migration of ooids became trapped onto a newly existing surface area of bedrock <6000BP, where possible microbial mat development could have aided in incoming sediment entrapment and further cementing lithification, allowing sediment accumulation to succeed sea level rise in the early Holocene.
5. Island growth occurs as per Figure 7.

Given the understanding of the described development of LAC as an interior island on a carbonate platform, utilizing data from core facies interpretations based on comparison settings, grain size and composition, roundness, and sorting, as well as lithofacies correlations based on age, I hypothesize that Little Ambergris Cay underwent a series of high to low energy facies changes supporting eastward accumulation. This information furthers the research of carbonate platform studies, and is applicable to the unconventional field search of petroleum (Dravis and Wanless, 2008), and the geochemical and geobiological studies of geology by providing a modern analogue of unique climatic, biological, physical and chemical conditions of carbonate platform interior island formation.

<u>References</u>:

AZoM.com. (2016). *What is the Effect of Sample Size on Particle Size Distribution Measurements?* [online] Available at: https://www.azom.com/article.aspx?ArticleID=12587 [Accessed 28 Oct. 2020].

Bernier, JC., "Data Dictionary for Grain-Size Data Tables" [online] available at: https://pubs.usgs.gov/ds/0834/data/Metadata/Tables_metadata/Cat_Island_grainsize_data%20dictionary.pdf

Broecker, Wallace S., et al. "Factors Controlling the Rate of CaCO3precipitation on Great Bahama Bank." *Global Biogeochemical Cycles*, vol. 15, no. 3, 2001, pp. 589–596., doi:10.1029/2000gb001350.

de Mahiques M.M. (2016) Sediment Sorting. In: Kennish M.J. (eds) Encyclopedia of Estuaries. Encyclopedia of Earth Sciences Series. Springer, Dordrecht. https://doi.org/10.1007/978-94-017-8801-4_348

data.world. (n.d.). *Cat Island marine core grain-size data from field ... 0BIM06 - dataset by us-doi-gov*. [online] Available at: https://data.world/us-doi-gov/67bc3fdc-0aed-4054-b75a-2d11e475819c [Accessed 28 Oct. 2020].

Diaz, Mara & Eberli, Gregor & Blackwelder, Patricia & Phillips, Brian & Swart, Peter. (2017). Microbially mediated organomineralization in the formation of ooids. Geology. 45. 771-774. 10.1130/G39159.1.

Diaz, Mara R., and Gregor P. Eberli. "Decoding the Mechanism of Formation in Marine Ooids: A Review." *Earth-Science Reviews*, vol. 190, 2019, pp. 536–556., doi:10.1016/j.earscirev.2018.12.016.

Dickson, J.A.D., and Arthur Saller. "Caicos Platform Shoals Formation and Erosion, Turks and Caicos Islands." *Developing Models and Analogs for Isolated Carbonate Platforms—Holocene and Pleistocene Carbonates of Caicos Platform, British West Indies*, 2008, doi:10.2110/pec.08.22.0133.

Dravis, Jeffrey J., and Harold R. Wanless. "Impact of Strong Easterly Trade Winds on Carbonate Petroleum Exploration - Relationships Developed from Caicos Platform, Southeastern Bahamas." *Marine and Petroleum Geology*, vol. 85, 15 Apr. 2017, pp. 272–300., doi:10.1016/j.marpetgeo.2017.04.010.

Dravis, Jeffrey J., and Harold R. Wanless, 2008. "Caicos Platform Models of Quaternary Carbonate Deposition Controlled by Stronger Easterly Trade Winds—Applications to Petroleum Exploration", Developing Models and Analogs for Isolated Carbonate Platforms—Holocene and Pleistocene Carbonates of Caicos Platform, British West Indies, William A. Morgan, Paul M. (Mitch) Harris

Dravis, Jeffrey J., and Harold R. Wanless, 1989. "Carbonate Environments and Sequences of Caicos Platform: Caicos, British West Indies to Miami, Florida", July 20 - 26, 1989, Volume T374

Duguid, Sarah Marie Anne. "Origin and geochemistry of modern Bahamian ooids." Queens University Masters Thesis, 2009, MR48176

Dutch, Rian & Krapf, Carmen & Curtis, Stacey & Nicolson, Benjamin & Pawley, Mark & Preiss, Wolfgang & Sheard, Malcolm & Werner, Mario. (2015). Geological Survey of South Australia glossary of Validated lithology modifier and landform terms used for digital field note capture.

Entegris. 2020. *What is the Effect of Sample Size on Particle Size Distribution Measurements?*. AZoM, viewed 27 October 2020, https://www.azom.com/article.aspx?ArticleID=12587.

Jamison-Todd, S., Stein, N., Overeem, I., Khalid, A., & Trower, E. J. (2020). Hurricane deposits on carbonate platforms: A case study of Hurricane Irma deposits on Little Ambergris Cay, Turks and Caicos Islands. *Journal of Geophysical Research: Earth Surface*, 125, e2020JF005597. https://doi.org/10.1029/2020JF005597

Jones, Gareth D., et al. "An Investigation of Early Diagenesis in an Isolated Carbonate Platform Caicos Platform, British West Indies." *Developing Models and Analogs for Isolated Carbonate Platforms—Holocene and Pleistocene Carbonates of Caicos Platform, British West Indies*, 2008, doi:10.2110/pec.08.22.0177.

Kerans, Charles, et al. "Anatomy of a Late Quaternary Carbonate Island: Constraints on Timing and Magnitude of Sea-Level Fluctuations, West Caicos, Turks and Caicos Islands, BWI." *Quaternary Science Reviews*, vol. 205, Jan. 2019, pp. 193–223., doi:10.1016/j.quascirev.2018.12.010.

Kaczmarek, Stephen & Hasiuk, Franciszek. (2008). Mapping surficial sediment distributions on Caicos Platform: A quantitative approach integrating statistical analysis of Landsat spectral data and field observations. 10.2110/pec.08.22.0057.

Kindler, Pascal, et al. "Pre-Holocene Island Geology of the Caicos and Mayaguana (Bahamas) Platforms Similarities and Differences." *Developing Models and Analogs for Isolated Carbonate Platforms—Holocene and Pleistocene Carbonates of Caicos Platform, British West Indies*, 2008, doi:10.2110/pec.08.22.0211.

Krumbein, W. C., 1940, Flood gravels of San Gabriel Canyon, California: Geological Society of America Bulletin, 51:639-676.

Neese, Douglas G., "OOID DIAGENESIS: HOLOCENE GEOCHEMISTRY OF THE ROCK/WATER/ATMOSPHERIC SYSTEM" University of Oklahoma Ph.D. Dissertation, 1986, 8611788

Orzechowski, E., Strauss, J., Knoll, A., Fischer, W., Cantine, M., Metcalfe, K., Quinn, D., Stein, N., Gomes, M., and Grotzinger, H., 2016, Age and construction of Little Ambergris Cay bedrock rim, southeastern Caicos Platform, British West Indies, in Proceedings American Geophysical Union Fall Meeting, San Francisco, California, 2016.

Ostling, Johanna L., et al. "The Biogeomorphology of Mangroves and Their Role in Natural Hazards Mitigation." *Geography Compass*, vol. 3, no. 5, 2009, pp. 1607–1624., doi:10.1111/j.1749-8198.2009.00265.x.

Powers, M.C., 1953, A new roundness scale for sedimentary particles: Journal of Sedimentary Petrology, 23:117-119.

Rankey, Eugene C., et al. "Geomorphology and Sedimentology of Ambergris Ooid Shoal, Caicos Platform." *Developing Models and Analogs for Isolated Carbonate Platforms—Holocene and Pleistocene Carbonates of Caicos Platform, British West Indies*, 2008, doi:10.2110/pec.08.22.0127.

Schlager, Wolfgang. (2003). Benthic carbonate factories of the Phanerozoic. International Journal of Earth Sciences. 92. 10.1007/s00531-003-0327-x.

Swart, P.k., et al. "The Fertilization of the Bahamas by Saharan Dust: A Trigger for Carbonate Precipitation?" *Geology*, vol. 42, no. 8, 2014, pp. 671–674., doi:10.1130/g35744.1.

Toscano, M.A. & Macintyre, I.G. 2003, "Corrected western Atlantic sea-level curve for the last 11,000 years based on calibrated 14C dates from Acropora palmata framework and intertidal mangrove peat", Coral Reefs, vol. 22, no. 3, pp. 257-270.

Trower, Elizabeth J., et al. "Active Ooid Growth Driven By Sediment Transport in a High-Energy Shoal, Little Ambergris Cay, Turks and Caicos Islands." *Journal of Sedimentary Research*, vol. 88, no. 9, 2018, pp. 1132–1151., doi:10.2110/jsr.2018.59.

Westphal, Hildegard, et al. "Carbonate Depositional Systems: Assessing Dimensions and Controlling Parameters." *Springer*, 2010, doi:10.1007/978-90-481-9364-6.